X-621-70-114

NONTHERMAL HEATING IN THE TWO-FLUID SOLAR-WIND MODEL

R. E. HARTLE
AARON BARNES

APRIL 1970

GSFC

GODDARD SPACE FLIGHT CENTER
GREENBELT, MARYLAND

NONTHERMAL HEATING IN THE TWO-FLUID SOLAR-WIND MODEL

by

R. E. Hartle
Laboratory for Planetary Atmospheres
NASA, Goddard Space Flight Center
Greenbelt, Maryland 20771

Aaron Barnes
Space Sciences Division
NASA, Ames Research Center
Moffett Field, California 94035

ABSTRACT

The two-fluid solar-wind model predicted values for wind speed and proton temperature that are lower than average observed values; however, the predictions are consistent with the empirical relation of Burlaga and Ogilvie in which the square root of the proton temperature is proportional to the wind speed. Since observed values of wind speed and proton temperature are typically higher than those of the two-fluid model, it is concluded that energy must be supplied by dissipation of nonthermal energy from an external source. The two-fluid model is therefore extended by including ad hoc an energy source in the proton heat equation whose strength and spatial distribution is varied to determine the general requirements of such a source. The main features of our results are: Heat deposited inside the heliocentric radius $r \simeq 4\ R_\odot$ results in a significant increase in wind speed with negligible increase in proton temperature. Depositing heat over the range $r \gtrsim 25\ R_\odot$ results in a large increase in proton temperature and negligible increase in wind speed. By depositing heat over the extended range $2\ R_\odot \lesssim r \lesssim 25\ R_\odot$, solar-wind speeds and proton temperatures can be brought in direct correspondence with the empirical results of Burlaga and Ogilvie. Based on this model we conclude that primary energy deposition should take place inside $r \simeq 25\ R_\odot$.

1. INTRODUCTION

In this paper we describe a simple two-fluid model of solar-wind flow which includes dissipation of nonthermal energy as well as thermal conduction. From its beginning, the theory of the solar wind has been concerned with the problem of energy transport in the solar corona [see reviews by Parker, 1969, 1965a, 1963]. The coronal gas is fairly tightly bound in the sun's gravitational field, so that if there is a solar wind, there must exist a heat source strong enough to lift the gas out of solar gravity. This heating must extend out from the sun at least as far as the critical distance (the distance at which the solar-wind flow becomes supersonic).

The mechanisms which provide the necessary heating are not yet understood in quantitative detail. Parker [1963, 1965a, b] has discussed in detail the possibility that the heat transport of the wind is entirely due to thermal conduction. He found that purely conductive models imply lower wind velocity and higher density than are observed at the orbit of earth (in fact, for a base temperature of $2 \times 10^{6\,\circ}K$, the observed coronal density of $\sim 10^{9}$ cm^{-3} implies subsonic expansion), a conclusion supported by the numerical calculations of Noble and Scarf [1963] and Whang and Chang [1965]. Parker suggested that at least two other effects may be important in solar-wind energetics: non-conductive heating, probably due to wave dissipation, and cutoff of thermal conduction, due either to spiraling of the interplanetary magnetic field or to some collisionless mechanism. Extended heating

in one-fluid models has been discussed in the polytrope approximation by Parker [1963]. Analytical discussions of one-fluid heating from several viewpoints have been given by Konyukov [1967a, b, 1968]. Konyukov's arguments are not completely convincing, however, especially as he incorrectly concludes that a purely conductive one-fluid model is unstable [Konyukov, 1968].

A more refined solar-wind model, where the only heat transport is classical heat conduction, is the two-fluid model [Sturrock and Hartle, 1966, Hartle and Sturrock, 1968], in which the distinct transport properties of electrons and protons are considered. This model predicts a flow speed of $\sim$250 km/sec and a proton temperature of $\sim 4 \times 10^3$ ^{o}K at the orbit of earth, considerably smaller than the typically observed values of $\gtrsim$ 350 km/sec and $\gtrsim 5 \times 10^4$ ^{o}K [Neugebauer and Snyder, 1966a; Wolfe et al, 1966; Axford, 1968, Hundhausen, 1968]; in addition, the two-fluid model predicts an electron temperature of $\sim 3.5 \times 10^5$ ^{o}K at 1 AU, larger than the observed value of $\sim 2 \times 10^5$ ^{o}K. It has been proposed that these deficiencies might be remedied by modifying this purely conductive model to include the possibility of heating by the dissipation of some nonthermal energy supply; several possible mechanisms have been discussed in the literature [Coleman, 1968; Barnes, 1969; Fredricks, 1969; Jokipii and Davis, 1969]. Recently, Hundhausen [1969] has suggested that inhibition of thermal conduction, rather than dissipation of nonthermal energy from some external source, may

account for the discrepancies between quiet-day observations and the predictions of the two-fluid model. Such inhibition of thermal conduction might be either a purely geometrical effect, associated with the spiraling of the interplanetary magnetic field [Brandt, et al, 1969; Gentry and Hundhausen, 1969; Urch, 1969], or a collisionless plasma effect, perhaps of the sort discussed by Forslund [1970].

Nevertheless, the observed solar wind often blows much faster than the quiet-day wind for periods of several days (e.g., see Neugebauer and Snyder, 1966a), so that the wind convects much more energy at some times than at others. This variability of the energy flux is almost certainly associated with the dissipation of varying amounts of nonthermal energy [Parker, 1969, 1965a]. This viewpoint is consistent with the strong observational correlation between the flow speed v_E and proton temperature T_{pE} of the wind at 1 AU [Burlaga and Ogilvie, 1970; Robbins et al, 1970]. In particular, Burlaga and Ogilvie find the empirical relation $T_{pE}^{1/2} = (.036 \pm .003)\ v_E - (5.54 \pm 1.50)$, where the proton temperature T_{pE} is in units of $10^3\ ^oK$ and the flow speed v_E is in km/sec. (subscript E refers to Earth's orbit throughout). This remarkable relation is valid for a wide variety of solar-wind conditions[1], ranging from quiet to highly disturbed times. There is also evidence for a weaker correlation between density and temperature [Robbins et al, 1970], especially for temperatures lower than $5 \times 10^4\ ^oK$ [Hundhausen, private communication].

[1] This relation is based on Explorer 34 plasma measurements made between June and December of 1967, but seems to agree with other observations made at other times in the solar cycle.

However, the T_{pE}-v_E correlation is much stronger [Robbins et al, 1970], and probably a more fundamental characteristic of solar-wind flow at the orbit of earth.

Since disturbed wind conditions often persist for several days (a time comparable to the time of flow between the sun and the orbit of earth), it seems likely that the Burlaga-Ogilvie T_{pE}-v_E relation defines a continuum of average macroscopic states of the solar wind,[1] rather than mere correlations in the microstructure of the wind; presumably, high velocities (and temperatures) indicate a state of the wind that has undergone extended heating. If this interpretation of the T_{pE}-v_E relation is correct, it has important implications for theoretical models of the wind. For example, most one-fluid models [Noble and Scarf, 1963; Whang and Chang, 1965; Gentry and Hundhausen, 1969, Urch, 1969] give values of flow speed and temperature that separately lie in the observed range, but do not satisfy the T_{pE}-v_E relation; accordingly, we conclude that none of these models describes an observed average state of the wind. On the other hand, the two-fluid model is consistent with extrapolation of the T_{pE}-v_E relation to low temperature and flow speed.

If the Burlaga-Ogilvie T_{pE}-v_E relation is a fundamental property of macroscopic solar-wind flow, it must be explainable by a sufficiently realistic model of the wind. Obviously, such a model must not simply predict a flow speed and proton temperature at (say) a heliocentric distance of 1 AU but rather it should predict a continuous range of T_{pE} and v_E consistent with the

empirical T_{pE}-v_E relation. In the present paper, we discuss a simple model which is consistent with the empirical T_{pE}-v_E relation; although this model does not actually predict the T_{pE}-v_E relation, we believe that it indicates some of the features that a predictive model must have. Our present model is similar to the two-fluid model in the form presented by Hartle and Sturrock [1968], but includes heating of the ions (but not electrons) by dissipation of nonthermal energy from an external source.[2] We do not specify the mechanism that supplies this nonthermal energy, but assume ad hoc an energy dissipation function which permits us to vary the strength and spatial distribution of the heating in a general way.

We solve the dynamical equations of solar-wind flow for various shapes and strengths of the energy deposition function. We find that heat deposited in the region of subsonic flow mainly raises the flow speed v_E at 1 AU, and heat deposited in the region of supersonic flow mainly raises the proton temperature T_{pE} at 1 AU.[3] By discarding solutions not consistent with the Burlaga-Ogilvie T_{pE}-v_E relation, we obtain a series of solutions which indicate that the external heat source has the following property: the primary heating occurs over an extended region, possibly as far as 25 $R_\odot$ from the sun; also, weaker heating may

---

[2]This model is fluid theory, as opposed to exospheric theories (e.g., Hollweg [1970], Eviatar and Schulz [1970], Jockers [1969]).

[3]This effect is not surprising, since the addition of heat to subsonic flow increases Mach number, while addition of heat to supersonic flow reduces Mach number [Shapiro, 1953].

occur much farther out ($\sim$ 1 AU), but has only a secondary influence, affecting the temperature but not the flow speed.

In the limit of zero energy deposition our solutions reduce to the basic two-fluid model.[4] Although this limit may not be an attainable state of solar wind flow, because the large ratio of electron to proton temperature may cause instability [Fredricks, 1969, Forslund, 1970], it is reasonable to use the two-fluid equations to investigate the effects of nonthermal energy deposition for two reasons: first, the addition of modest amounts of heat raises the proton temperature high enough that the strongest instabilities considered by Fredricks and Forslund do not occur; second, as mentioned before, extrapolation of the empirical T_{pE}-v_E relation to low velocity and temperature is consistent with the basic two-fluid model, suggesting that it is a reasonable mathematical zero-heating limit of the models with finite heating.

Hundhausen [1969] has emphasized that the two-fluid model implies a thermal conduction flux considerably higher than that deduced from electron measurement at 1 AU [Montgomery et al., 1968]. He suggested that this may mean that the transport coefficients of the two-fluid model become invalid at some point in the flow; this possibility had already been mentioned briefly by Hartle and Sturrock [1968] and has been discussed in considerable detail by Forslund [1970]. It is clear that inhibition of

---

[4] One cannot produce the T_{pE}-v_E relation by variation of the base parameters of the two-fluid model. This was shown by numerical computation, and also may be seen from the approximate equations (5.1) of Hartle and Sturrock [1968].

thermal conduction, by whatever mechanism, is an effect which should be taken into account in a realistic model of the minimum solar wind. However, it is doubtful that inhibition of thermal conduction is related to the wide variation in energy flux associated with various macroscopic states of the solar wind. This kind of effect has been omitted from the present model, and probably does not modify our qualitative conclusions in a significant way.

Hundhausen [1969] has also raised the point that the two-fluid model predicts a total energy flux at 1 AU which is larger than the observed quiet-day flux by a factor ~2. This may not be a fundamental difficulty of the two-fluid model, for the total efflux of energy in the quiet-day wind is a fairly small fraction (~ 10%) of the heat required to drive the wind (most of this heat goes into work of lifting the plasma out of solar gravity), so that a small error in describing the heating process may cause a rather large error in the net energy flux in the distant flow. Further, the observational correlation between temperature and flow speed is much stronger than that between either of these quantities and density, so that density (and hence energy flux, whose convective part is proportional to density) may not be a critical test of a solar-wind model [cf. also Parker, 1965a].

2. BASIC EQUATIONS AND THEIR SOLUTION

To make the calculations tractable we assume that the solar wind consists of protons and electrons and undergoes steady, radial, spherically symmetric expansion characterized by a proton number density n and flow speed v (equal to the electron density and flow speed), proton temperature T_p and electron temperature T_e. Effects of solar rotation, magnetic field, temperature anisotropy and viscosity are ignored. The equations that govern the flow are the continuity equation

$$n\ v\ r^2 = J = \text{constant} \tag{1}$$

(r is the heliocentric distance), the momentum equation

$$n\ m_p\ v\ \frac{dv}{dr} = -\frac{d}{dr}\ [nk(T_e + T_p)] - \frac{G\ M_\odot\ m_p\ n}{r^2} \tag{2}$$

and the electron and proton energy equations

$$\frac{3}{2}\ n\ v\ k\ \frac{dT_e}{dr} - v\ k\ T_e\ \frac{dn}{dr} - \frac{1}{r^2}\ \frac{d}{dr}\left(r^2\ \kappa_e\ \frac{dT_e}{dr}\right) =$$

$$-\frac{3}{2}\ \nu_E\ nk(T_e - T_p) + \wp_e \tag{3}$$

$$\frac{3}{2}\ n\ v\ k\ \frac{dT_p}{dr} - v\ k\ T_p\ \frac{dn}{dr} - \frac{1}{r^2}\ \frac{d}{dr}\left(r^2\ \kappa_p\ \frac{dT_p}{dr}\right) =$$

$$\frac{3}{2}\ \nu_E\ n\ k(T_e - T_p) + \wp_p \tag{4}$$

(the $\wp$'s are unspecified collisionless heating terms).

Here m_p and m_e are, respectively, the proton and electron masses, G is the gravitational constant, $M_\odot$ is the mass of the sun, k is Boltzmann's constant,

$$\kappa_e = 3.16 \frac{n\, k^2\, T_e}{m_e \nu_e} \tag{5}$$

and

$$\kappa_p = 3.9 \frac{n\, k^2\, T_p}{m_p \nu_p} \tag{6}$$

are the electron and proton collisional thermal conductivities,

$$\nu_E = \frac{2m_e}{m_p} \nu_e \tag{7}$$

is the collisional electron-proton energy exchange rate,

$$\nu_e = \frac{4(2\pi)^{1/2}\, n\, e^4\, \lambda}{3\, m_e^{1/2} (k\, T_e)^{3/2}} \tag{8}$$

and

$$\nu_p = \frac{4\pi^{1/2}\, n\, e^4\, \lambda}{3\, m_p^{1/2} (k\, T_p)^{3/2}} \tag{9}$$

are the electron and proton collision frequencies, and

$$\lambda \equiv \ell n\ \Lambda \equiv \ell n \left[\frac{3(k\ T_e)^{3/2}}{2\pi^{1/2}\ e^3\ n^{1/2}} \right] \qquad (10)$$

is the Coulomb logarithm. The expressions for the collisional transport terms are taken from the review article by Braginskii [1965].

Equations (1-10) are the same as the basic equations used by Hartle and Sturrock [1968; hereafter called HS] except for the collisionless heating terms $\mathcal{P}_e$ and $\mathcal{P}_p$ in equations (3-4). It is proper to treat the collisionless heating by additive terms, as corrections to the particle kinetic equations due to collisionless effects (wave-particle interactions) are additive (e.g., see Rogister and Oberman, [1968]). In principle the momentum equation (2) (but, obviously, not the continuity equation (1))has an additional term due to collisionless effects, a pressure-like term analogous to radiation pressure. However, one may argue on physical grounds that this collisionless acceleration is not a major effect, and that the collisionless processes influence acceleration only through modifying proton and electron temperatures according to the heat equation. For suppose that the collisionless heating is due to some kind of dissipation of fluctuations of energy density $\mathcal{E}$, which move with speed u relative to the wind, and that u is comparable to the proton thermal speed or Alfvén speed; the momentum density of the fluctuations is of order $\mathcal{E}/(u+v)$. The corresponding gas energy density appearing in the heat equations is of the

order of the pressure $P = nk(T_e + T_p)$, and the related gas momentum density is of order $P/v + m_p nv$. We estimate the importance of the collisionless terms in the heat equations by the ratio η of the energy flux of the fluctuations to the gas energy flux appearing in the heat equations,

$$\eta \sim \frac{\mathcal{E}(u + v)}{Pv} = \frac{\mathcal{E}}{p} (1 + u/v) .$$

If η is of order 0.1 or larger, we expect collisionless heating to be important in the dynamics of the wind. Similarly, we estimate the importance of collisionless terms in the momentum equation by the ratio

$$\mu \sim \frac{\mathcal{E}}{u+v} (u+v) \frac{1}{P+m_p nv^2} \sim \frac{\eta}{(1+u/v)\ (1+m_p nv^2/P)} .$$

It is clear that $\mu << \eta$ both in the subsonic-flow region, where $u >> v$ and $m_p nv^2 << P$, and in the supersonic-flow region, where $u << v$ and $m_p nv^2 >> P$. Hence collisionless processes are much less significant for acceleration than for heating (except possibly in the small region of subsonic-supersonic transition), and terms describing collisionless acceleration need not appear in equation (2).

The solutions of the dynamical equations (1-4) depend on the forms of the collisionless heating terms $\mathcal{P}_e$ and $\mathcal{P}_p$. In the present work we <u>assume</u> that $\mathcal{P}_e = 0$ and

$$\mathcal{P}_p = D_o \left(\frac{n}{n_o}\right) \exp \left[- \frac{(r/R_\odot - a)^2}{b^2} \right] \qquad (11)$$

D_o is a measure of the strength of collisionless heating ($D_o = 0$ corresponds to the bare two-fluid equations of HS), a is the heliocentric distance (in $R_\odot$) of maximum energy deposition, b is the spread of the energy deposition, and n_o is the proton number density at the base of the model $r = r_o$. The total energy deposition rate by collisionless processes in the wind between the base of the corona and heliocentric distance r is

$$\Delta E(r) = 4\pi D_o \int_{R_\odot}^{r} \left(\frac{n(\rho)}{n_o}\right) \exp\left[-\frac{(\rho/R_\odot - a)^2}{b^2}\right] \rho^2 \, d\rho \qquad (12)$$

which must be computed numerically from the solutions of the dynamical equations. We emphasize that equations (11) and (12) are not realistic descriptions of the energy deposition; the form (11) was chosen because the exponential term permits straightforward investigation of the qualitative effects of heat sources of various strengths, locations and spreads, and the factor (n/n_o) permits a simple dependence of the heating on the amount of matter present.

Except for the specification of the heating strength D_o, its position a, and its spread b, the boundary conditions are the same as in HS. We specify the base density and temperatures n_o, T_{e0}, T_{p0}, require that T_e and T_p tend to zero as r goes to infinity, and that the solar-wind velocity should pass continuously through a subsonic-supersonic transition.

The dynamical equations (1-4) are solved numerically by the iterative technique of HS. We begin by guessing the temperature

profiles $T_e(r)$ and $T_p(r)$, and use them to solve the momentum equation (2) (from which the density has been eliminated via (1)). There is a unique solution of equation (2) which exhibits the required subsonic-supersonic transition; this velocity profile $v(r)$, together with the base density n_o, give the density profile $n(r)$ according to equation (1).

We then use the values of $v(r)$ so computed, together with the assumed $T_p(r)$, to solve the electron heat equation (3) for $T_e(r)$, subject to the boundary conditions on T_e at $r = r_o$ and $r = \infty$. The outer boundary condition is handled by requiring that $T_e(r)$ exhibit the asymptotic dependence $T_e(r) \propto r^{-2/7}$ at large r; this asymptotic form obtains because the conduction term dominates the electron heat equation at large r. Having calculated $n(r)$, $v(r)$ and $T_e(r)$, we use these data to solve the proton heat equation (4) for $T_p(r)$, subject to the boundary condition on T_p at $r = r_o$. This equation is essentially a first-order equation beyond a few solar radii, because the heat exchange term dominates the proton conduction term. In this case, $T_p(r) \propto r^{-6/7}$ as $r \to \infty$ because of the dominance of the energy exchange term and the $r^{-2/7}$ dependence of T_e.

This sequence of calculations, which began with assumed values of $T_e(r)$ and $T_p(r)$, has yielded new functions T_e and T_p satisfying the boundary conditions. These may be used to solve the equation of motion again and so repeat the previous cycle. This cyclic process is repeated until the changes in the variables from one cycle to the next are so small as to be judged in-

significant. To this approximation, all equations and boundary conditions are satisfied. Further details of the solution procedure are discussed in HS.

The introduction of the heating term (11) into the two-fluid model calculation introduces essentially no new element into the computation procedure. However, in order to get good first "guesses" of the temperature profiles, it is convenient to generate a series of models, beginning with a bare two-fluid model ($D_o = 0$), then gradually raising D_o in steps, using in each step the temperature profiles computed in the previous step as the basis for choosing the first trail temperature profiles for the iterative solution of the dynamical equations.

3. ANALYTICAL RESULTS

The principle model of HS, chosen on the basis of a close fit to the observed coronal density profile of Blackwell [1956], required $n_o = 3 \times 10^7 cm^{-3}$ and $T_{eo} = T_{po} = 2 \times 10^6\ ^oK$ at a base radius $r_o = R_\odot$. We have used this model as a point of departure to determine the effects of collisionless proton heating. However, we have taken a base radius r_o of $2R_\odot$ to avoid the necessity of including the complications due to strong small scale magnetic fields and attendant non-radial expansion expected to be important inside this point. Then, for this case, the derived base values of HS we have used are: $n_o = 1.5 \times 10^6\ cm^{-3}$, $T_{eo} = 1.5 \times 10^6\ ^oK$, and $T_{po} = 1.2 \times 10^6\ ^oK$.

We have divided the analysis into two classes based on the parameters of the assumed density weighted gaussian heat source given by equation (11). In the first class, the half width b is held fixed while the central position of the gaussian a ($a > 5$) and the amplitude factor D_o are allowed to vary. In the second class, a is fixed at 2 while b and D_o are varied. The first class of models corresponds to energy deposition almost all of which takes place well above the base while the second class corresponds to heating over a finite range extending from the base. To determine the significance of each model in a given class, with heat source characterized by (a,b,D_o), we compare the corresponding proton temperature T_{pE} and wind speed v_E at Earth's orbit with the empirical relation of Burlaga and Ogilvie discussed above.

The analytical results of the first class of models are shown parametrically by the solid lines (and their extensions shown by dotted lines) in Figure 1 where the square root of the proton temperature at 1 AU in kilo-degrees Kelvin is plotted against the corresponding wind speed in km/sec. The resulting density n_E is indicated at selected points along the curve. The dashed lines are the empirical results of Burlaga and Ogilvie, where the central dashed line, given by $T_{pE}^{1/2} = 0.036v_E - 5.54$, represents the average values and the outer dashed lines, given by $T_{pE}^{1/2} = (0.036 \pm 0.003)\ v_E - (5.54 \pm 1.50)$, represent their variance. In this series, the half width b is fixed at 5 while each individual curve corresponds to a fixed central position a. Then, upon increasing the rate of energy deposition by increasing D_o from zero, for a given a and b, the solution points move upward from the basic solution of HS indicated at the apex of the curves.

For completeness, the values of the amplitude factor D_o corresponding to solution points designated by the density values and listed in an order starting with the basic HS solution are: for a = 6, $D_o \times 10^8 = 1, 1.5$; for a = 9, $D_o \times 10^8 = 0.5, 1, 1.5, 2.5$; for a = 12, $D_o \times 10^8 = 0.2, 0.6, 1, 1.5, 2$; for a = 16, $D_o \times 10^8 = 0.3, 0.7, 1, 1.3$; for a = 20, $D_o \times 10^8 = 0.44, 0.97, 1.2$; for a = 30, $D_o \times 10^8 = 0.24, 0.58$. For example, when a = 12 and v_E = 340 km/sec we note that $D_o = 1.5 \times 10^{-8}$. The total energy deposition rate $\Delta E\ (\infty)$ of equation (12) can be determined to a good approximation by

taking the difference between the streaming energy rate (at 1 AU) and the corresponding rate of the HS model without heating.

Some of the results shown in Figure 1 are not consistent with the assumption of a local maxwellian velocity distribution implicitly required by the basic equations (2) through (4). Local thermodynamic equilibrium is maintained when the proton momentum and energy relaxation rates ν_p, given by equation (9), are greater than the characteristic expansion rate $\nu_{exp} = -(v/n)(dn/dr)$. The analytical results lying in the region where equilibrium is not expected to be maintained by Coulomb collisions, i.e. $\nu_p < \nu_{exp}$, are indicated by dotted lines. Then, the results lying in the range of observation with wind speeds greater than about 320 km/sec and proton temperatures greater than 3×10^4 ^oK are not to be relied upon in the strictest sense. The results lying in the observed range with v_E somewhat greater than 320 km/sec and T_{pE} somewhat greater than 3×10^4 ^oK are to be regarded as preliminary estimates to solutions of an appropriate kinetic equation required in this region.

In every case shown in Figure 1, for sources of fixed spread b and position a, the solar wind speed v_E and proton temperature T_{pE} increase while the density n_E decreases when the heating rate is increased (by increasing D_o). More importantly, this same variation is noted for those solution points consistent with the empirical relation of Burlaga and Ogilvie. In this case, the central position a is constrained to move inward toward the

sun while the heating rate is increased. That is, if D_o is increased and a is decreased in a specified manner so that solution points lie on the central dashed line then v_E and T_{pE} increase while n_E decreases. In this case, we find that the amplitude D_o varies as the inverse square of the central position a over the range 275 km/sec < v_E < 400 km/sec. The decrease in density n_E is desirable since densities observed when v_E > 250 km/sec are usually lower than the 15 cm^{-3} resulting from the model of HS without heating.

At this point we conclude that to attain solar wind speeds, say, greater than 300 km/sec while simultaneously maintaining proton temperatures low enough to agree with observation the primary energy deposition must take place within a heleocentric radius of about 25 R_o (see results for a = 16, 12, and 9 in Figure 1). Heating outside this range produces primarily an increase in proton temperature T_{pE} with negligible increase in wind speed v_E as indicated in Figure 1 when a = 30. To further establish this conclusion, we have investigated the effects of varying the spread b, the base temperature T_{po}, and the base density n_o.

Upon varying the half width b over the range $1 \leq b \leq 9$, while keeping a and D_o fixed, we find that solution points in the observational range move approximately along the corresponding curves of constant a in Figure 1. That is, increasing (decreasing) b corresponds to an increase (decrease) in v_E and T_{pE} as the point ($T_{pE}^{1/2}$, v_E) moves along a curve of constant a. This

result follows since an increase or decrease in b implies an increase or decrease, respectively, in the rate of energy deposition. The corresponding variation of density n_E is negligible for the range of b considered. For example, when $a = 12$ and $D_o = 10^{-8}$, an increase in b from 5 to 9 results in an increase in v_E from 320 km/sec to 340 km/sec, an increase in T_{pE} from 2.8×10^4 °K to 5.0×10^4 °K while the density n_E remains constant at 11 cm^{-3}. However, since n_E remains essentially constant while v_E and T_{pE} increase (as b increases) along a curve of constant a, we note that at a given point $(T_{pE}^{1/2}, v_E)$ in Figure 1 there will be a slight increase in the corresponding value of n_E.

In many treatments of the solar wind [Parker, 1963, 1965a, 1969; Noble and Scarf, 1963; Brandt et al., 1965] it is usually concluded that a heat source is necessary between $1R_\odot$ and $2R_\odot$ in order that derived coronal density distributions in this region can be made to fit the observed distributions. In this case, the base temperature $T_{po} = 1.2 \times 10^6$ °K at $r_o = 2R_\odot$, used in the above, may be too low. The truth of this, of course, is dependent upon the base temperature at $1R_\odot$ and the degree of heating required between $1R_\odot$ and $2R_\odot$. We have examined the effects of increasing the base temperature T_{po} at $2R_\odot$ for values of a, b, and D_o corresponding to solution points of Figure 1 in the range of observation. In each case, an increase in T_{po} from 1.2×10^6 °K to 1.5×10^6 °K (the value of T_{eo}) resulted in an increase in the density n_E while the remaining parameters v_E, T_{pE}, and T_{eE} remained essentially unchanged. For example,

increasing T_{po} from 1.2×10^6 °K to 1.5×10^6 °K with a = 12, b = 5, and $D_o = 1.5 \times 10^{-8}$ leads to an increase in n_E from 11 cm^{-3} to 16 cm^{-3} while v_E and T_{pE} remain constant at 340 km/sec and 4.5×10^4 °K, respectively, Therefore, the essential change required in Figure 1 when the base temperature is 1.5×10^6 °K instead of 1.2×10^6 °K is an increase in the indicated values of the density.

We have thus shown that the conclusion above stating that a primary heat source must be placed within about $25R_\odot$ to attain wind speeds greater than 300 km/sec remains unchanged when b and T_{po} are allowed to vary over the above mentioned ranges. The increase in density n_E at a given point $(T_{pE}^{1/2}, v_E)$, resulting from an increase in b or T_{po}, can be reduced by decreasing the base density n_o. We find that a decrease in n_o, for a given a and D_o, results in an increase in v_E and T_{pE} with a corresponding decrease in n_E in the range of observations. As occured when b was varied, the solution points $(T_{pE}^{1/2}, v_E)$ approximately follow curves of constant a. The increase in T_{pE} as n_o is reduced is contrary to the result obtained in the model without heating (T_{pE} decreased). This increase in T_{pE}, when a heat source is applied, is due to the fact that as n_o is decreased (and concomittently decreasing n(r), for $r > 2R_\odot$) there is effectively more energy deposited per proton, part of which appears as an increase in the proton temperature.

Having established the importance of heating inside $25R_\odot$, consider the second class of models displayed in Figure 2, where energy deposition takes place over a finite range extending from

the base. We have used the same representation as in Figure 1, in which case the solid lines are the theoretical results and the dashed lines are the empirical results. As before, the dotted lines are the analytical results lying in the region where pressure isotropy is not expected to be maintained by Coulomb collisions. In this series, solution points move from the basic solution without heating to higher values of $T_{pE}^{1/2}$ and v_E along curves of constant b as the heating rate is increased by increasing D_o from zero. The values of the amplitude factor D_o for the solutions indicated by the density values and listed in an order starting with the HS solution are: b = 2, $D_o \times 10^7$ = 0.3; 1.3; for b = 10, $D_o \times 10^8$ = 1, 1.5, 3; for b = 14, $D_o \times 10^8$ = 0.4, 1.5, 2, 2.5; for b = 18, $D_o \times 10^8$ = 0.2, 0.6, 1, 1.5; for b = 22, $D_o \times 10^9$ = 1, 4, 6, 8, 10; for b = 26, $D_o \times 10^9$ = 1, 3, 4, 6.

The essential conclusions drawn from Figure 1 can be obtained from Figure 2 except in the instance where heating takes place close to the base as indicated by the solution curve for b = 2. In this case, when the extent of the region of the energy deposition is effectively restricted to within $2R_\odot$ from the base, we note that not only are the proton temperatures much lower than observed but that there is an undesirable increase in the density above that of the basic model without heating. This density increase occurs because the heating is not sufficiently extended to yield the higher wind speeds associated with lower densities.

Then, increasing the extent of the heat source from the base, depicted by the remaining solutions in Figure 2, results in a

decrease in n_E and an increase in the corresponding values of v_E and T_{pE} when D_o is increased. As with the first class of models, there is a simple relation between the parameters of the heat source for corresponding solution points falling on data points; namely, D_o varies as the inverse fourth power of b over the range 275 km/sec < v_E < 400 km/sec. Densities n_E corresponding to v_E and T_{pE} in the range of observation are somewhat higher in the second class of models, pointing to the richness in the number of possible heating models. In addition, variations in T_{pE}, T_{eE}, v_E, and n_E resulting from variations in n_o and T_{po} are qualitatively similar to those occuring in the first class of models.

To further elucidate the preceding results, let us consider a few examples of temperature, density, and speed profiles which are consistent with the empirical results. Due to obvious limitations, we present only a few typical cases of the second class of models (heating over a finite range extending from the base). The conclusions drawn from this class will be applicable to the first class. Specificially, we consider the two cases in Figure 2 corresponding to: a = 2, b = 26, $D_o = 3 \times 10^{-9}$, $T_{pE} = 2.7 \times 10^4$ ^oK, $T_{eE} = 3.4 \times 10^5$ ^oK, v_E = 300 km/sec, $n_E = 13$ cm^{-3}; a = 2, b = 22, $D_o = 6 \times 10^{-9}$, $T_{pE} = 3.7 \times 10^4$ ^oK, $T_{eE} = 3.4 \times 10^5$ ^oK, v_E = 320 km/sec, $n_E = 13$ cm^{-3}.

The electron and proton temperatures for these models, as functions of heleocentric radii, normalized to one solar radius, are shown by solid lines in Figure 3. For comparison, the results

of the principle model of HS without heating are indicated by dashed lines (as will be done hereafter). The new results for the electron temperature T_e have not been shown since they are only slightly lower than found in the principle model (e.g., $T_{eE} = 3.4 \times 10^5\ ^oK$ in both cases); the lower temperatures are due to an increase in expansive cooling above that of the basic model. The proton temperatures in both models are elevated above those of the basic model, in direct response to the heat sources extending from the base. In each case, the proton temperature declines monotonically, although becoming almost isothermal around $10R_\odot$. (In the models of the first class, the temperature profiles are not always monotonic due to their response to the position and shape of the heat sources.) Of the two examples shown, that corresponding to the upper proton temperature curve lead to the higher wind speed at 1 AU due to the larger overall pressure gradient (the corresponding densities are about the same), resulting in greater acceleration. These temperature profiles serve to remind us that the higher temperatures T_{pE} and wind speeds v_E, agreeing with observation, correspond to overall energy deposition closer to the sun; i.e., as T_{pE} and v_E increase, the half width b decreases (and correspondingly D_o increases).

In the basic model without heating, proton thermal conduction was essentially unimportant beyond a few solar radii from the base. However, when heating takes place, proton thermal conduction is important to greater distances from the base due to the elevated

proton temperature along with the strong temperature dependence of the conduction coefficient. In particular, for the examples shown in Figure 3, proton thermal conduction accounted for about 20% of the proton energy flux out to 25-30$R_\odot$ from the base. Beyond this point it becomes unimportant and only thermal convection and expansive cooling are important. At several hundred astronomical units and beyond, thermal convection, expansion cooling, and energy exchange are dominant processes and $T_p \rightarrow r^{-6/7}$ as $r \rightarrow \infty$.

Figure 4 gives the density and speed profiles for the two examples shown in Figure 3. As noted previously, the example with the highest wind speed corresponds to the case of highest energy deposition leading to the greatest pressure gradiant and acceleration near the base. The density distributions for both cases are about the same, although somewhat lower than that of the basic model. It is worth noting in Figures 1 and 2 that the densities n_E, lying in the range of observation with $v_E \gtrsim 300$ km/sec, are essentially constant for a given class of models. The density decrease near the base, relative to the basic model, is permissible as can be noted in Figure 5 where the theoretical density distribution is compared with coronal density observations at solar minimum reported by Blackwell [1956], Michard [1954], and Allen [1963] and the representative distribution by Newkirk [1967].

The effects of raising the base proton temperature T_{po} are shown in Figure 6 and 7, where the case corresponding to

$D_o = 3 \times 10^{-9}$, a = 2, and b = 26 is considered. The dot-dashed lines in these figures result when $T_{po} = 1.5 \times 10^6$ °K while, for comparison, the solid lines are based on $T_{po} = 1.2 \times 10^6$ °K. The increase in proton temperature at the base, resulting in an increase in the pressure gradient near the base, leads to a higher base wind speed and corresponding larger particle flux. However, as mentioned above, the proton and electron temperatures and wind speed are essentially unchanged at 1 AU while the density is increased to 20 cm^{-3} (to maintain constant particle flux). The model with higher particle flux has lower acceleration near the base since more particles must be accelerated with less energy available per particle. The undesirable high density at 1 AU can be reduced by decreasing the base density. For example, a base density $n_o = 8.5 \times 10^5$ cm^{-3} leads to $n_E = 10$ cm^{-3}, with $v_E = 330$ km/sec, $T_{pE} = 4.9 \times 10^4$ °K, and $T_{eE} = 3.4 \times 10^5$ °K. Much further density decreases at the base leads to poor fits to the observed coronal density distributions ($2\text{-}20R_\odot$).

In the preceeding, the effects of viscosity were ignored. Due to low proton temperatures, viscosity is negligible in the HS model without heating. However, when heating takes place, viscous terms become larger as the proton temperature rises since the coefficient of viscosity varies as $T_p^{5/2}$. We have estimated the effects of adding viscous terms [see Braginskii, 1965] to the momentum and heat equations by treating them as small corrections and deriving their values from corresponding preceeding temperature and velocity profiles [n-th profiles; see Hartle

and Sturrock, 1968] in the iterative sequence. We find that collisional viscosity leads to small corrections for those cases corresponding to the upper portions of the solid lines ($\nu_p > \nu_{exp}$) in Figures 1 and 2. For example, considering the upper ends of the solid lines, we find that for the range $v_E \sim 275$ km/sec to ~ 375 km/sec the proton temperature increases ~10% to ~15% and v_E decreases slightly ($\lesssim 2\%$) when the viscous terms are included (a consequence of the fact that viscous heating is greatest for $r \gtrsim 30\ R_\odot$). Below the endpoints of the solid lines, towards lower temperatures, the viscous corrections diminish. For those solution points with $\nu_p < \nu_{exp}$ (dotted lines) in the observational range, corresponding viscous corrections are somewhat larger and result in an increase in T_{pE} by a factor of about 2-3 when v_E is high, 350-375 km/sec. However, Parker [1965a] has noted that when collisions are rare the viscous coefficient should be reduced by a factor $(r/\lambda)^2$, in terms of the collision mean-free path λ; hence, the above mentioned increase in T_{pE} by a factor of about 2-3 is an overestimate. With these considerations, we note that viscous corrections are not large over the parameter range of interest and that conclusions made above are essentially unaltered.

4. SUMMARY AND CONCLUSIONS

We have argued, as others have, that observed solar wind speeds and proton temperatures above those of HS suggest the need for additional energy transport across the base of the model, possibly in the form of waves which then deposit their energy in the system by means of collisionless damping. To account for such nonthermal energy deposition, we have taken a phenomenological approach by adding ad hoc a heat source to the proton heat equation without relating it to any particular mechanism. An electron heat source was not included. For ease of analysis and interpretation, the form of the proton heat source used was a density weighted gaussian given by equation (11). The base of the model was taken at $2R_\odot$ where corresponding values of temperature and density obtained by HS were used as boundary conditions. The empirical relation between v_E and T_{pE} determined by Burlaga and Ogilvie [1970] was used as a constraint on the parameters describing the heat source.

In every case considered, we found that, when the amplitude of the heat source with a given width and position was increased from zero, the wind speed v_E and proton temperature T_{pE} increased while the electron temperature T_{eE} decreased slightly from their respective values obtained in the HS model without heating (the estimates of v_E and T_{pE} in the HS model are in good accord with the corresponding values determined from the empirical relation of Burlaga and Ogilvie). In most instances, when the intensity of the heat source was raised, the density n_E was found to decrease

from 15 cm^{-3} obtained in the HS model; however, when energy deposition took place essentially within $2R_\odot$ from the base, the density increased from 15 cm^{-3} when the intensity of the heat source increased.

More specifically, upon comparing the variations of v_E and T_{pE} with the corresponding results from the empirical relation of Burlaga and Ogilvie, we find that an increase in the energy deposition rate, with deposition taking place beyond about $30R_\odot$ from the base, results in a significant increase in T_{pE} from the HS result and a negligible increase in v_E. In this case, upon increasing the heating rate, n_E does not decrease more than 7% from the 15 cm^{-3} of HS. In the opposite extreme, relative to the results of Burlaga and Ogilvie, v_E increases substantially while T_{pE} rises slightly when the heating rate is increased in sources depositing energy within $2R_\odot$ from the base. With such an increase in the heating rate the corresponding density n_E increases more than 30% above 15 cm^{-3}. However, when the primary energy deposition takes place within the range of approximately $2R_\odot$ to $25R_\odot$ from the base we showed that v_E and T_{pE} can be brought into direct correspondence with the empirical results of Burlaga and Ogilvie (over the range 275 km/sec $< v_E <$ 400 km/sec, $10^4\ ^oK < T_{pE} < 8\times10^4\ ^oK$) when suitable variations in the parameters of the heat source are made. In particular, refering to the heat source of equation (11), such correspondence obtains when $D_o \propto b^{-4}$ with $a = 2$, and $D_o \propto a^{-2}$ with $b = 5$ (of course, other parametric relations are possible). The corresponding proton density at

Earth's orbit ranged from 11 cm^{-3} to 13 cm^{-3}, a reduction of 12% to 25% below the value obtained by HS. Such a reduction is desirable since the observed average density is about 5-6 cm^{-3}; however, the observed density is known to range from 1 cm^{-3} to 30 cm^{-3} [Neugebauer and Snyder, 1966b; Wolfe et al, 1966; Lazarus et al, 1966; Gringauz, 1966].

Based on these considerations, we concluded, in the context of a two-fluid, spherically symmetric solar wind model, that primary energy deposition should take place inside about $25R_\odot$ from the base to obtain the more commonly observed wind speeds $v_E \gtrsim 275$ km/sec while simultaneously maintaining corresponding values of T_{pE} low enough to agree with data. Parker [1963, 1969] and Burlaga and Ogilvie [1970] have also suggested the need for an energy source in this region. This result is consistent with the nonthermal heating models recently proposed by Barnes [1969] and Fredricks [1969]. On the one hand, Barnes has proposed that the collisionless damping of fast-mode hydromagnetic waves propagating outward from below the base will deposit most of their energy into the proton (and electron) gas within $25R_\odot$. On the other hand, the turbulent ion-acoustic wave heating model proposed by Fredricks is operative over the range $20R_\odot$ to $60R_\odot$ when the conditions of the HS model prevail. In the Fredricks model ion-acoustic waves are generated (becoming unstable when $T_e/T_p \gtrsim 7$-10) by compressive MHD perturbations which could originate in part below the base (thereby constituting an external source). Based on the preceeding, the proton heating mechanism proposed by Barnes

is expected to be more significant since it is operative over more of the important range $2R_\odot \lesssim r \lesssim 25R_\odot$ while that of Fredricks is only operative over the outer end of this region. In addition, after some heating has occurred, the inner boundary of the Fredricks model, $r \simeq 20R_\odot$, will move out further to satisfy $T_e/T_p \gtrsim 7\text{-}10$ while proton heating in the Barnes model over the range $2R_\odot \lesssim r \lesssim 25R_\odot$ is expected to be more effective when $\beta_+ = 8\pi\, n\, k\, T_p/B^2$ is increased.

Even though we have shown that it is possible to obtain accord with the empirical relation between v_E and T_{pE} by application of energy sources over the region $2R_\odot \lesssim r \lesssim 25R_\odot$, we wish to make it clear that we do not rule out the possible importance of heating over the range $r \gtrsim 25R_\odot$. For example, consider the solid curves in Figures 1 and 2 lying well below the empirical results of Burlaga and Ogilvie. It can be shown that solution points on these curves can be raised essentially vertically to obtain correspondence with observation by an additional heat source depositing energy <u>anywhere</u> over the range 0.12 AU $\lesssim r \lesssim$ 1 AU. Of course, the bulk of the heating still takes place inside $25R_\odot$. For such an "extended" or "double-humped" heating model the corresponding densities n_E do not change noticably from their original, somewhat high values as the solution points are raised upward towards higher T_{pE} when a heat source is applied beyond $25R_\odot$.

If a small amount of heating beyond $25R_\odot$ ($\approx$1-5% of total energy) is actually required to raise T_{pE}, then the turbulent ion-acoustic heating model of Fredricks, also operative in this

region, may be important. In addition, two other possible external heating mechanisms in this region have been proposed by Coleman [1968] and Jokipii and Davis [1969]. Jokipii and Davis pointed out that the observed hydromagnetic wavelengths $\lesssim 10^7$ km are probably generated in the solar wind by the "collision" of fast and slow streams. The hydromagnetic waves generated then heat the protons locally through the collisionless damping mechanism of Barnes [1966]. We point out that such a hydromagnetic heating process in the very low β^+ streams of the HS model would be relatively insufficient and therefore the cooler streams should arrive appropriately pre-heated at the point of "collision" for the Jokipii and Davis model to be of significance. Coleman, on the other hand, has suggested that energy extracted from differential streaming motion cascades down through a hierarchy of turbulent eddies to those approximately the dimensions of a proton Larmor radius at which point dissipation takes place by proton cyclotron heating. However, Burlaga and Ogilvie [1970] have observed local heating or "hot spots" in the vicinity of positive velocity gradients but not negative gradients and therefore conclude that the heating is not a result of velocity shear but due to the collision of fast and slow streams. They also noted that the velocity gradients and corresponding "hot spots" occur infrequently and therefore the associated heating mechanism is not a dominant large scale phenomenon.

Proton heating in the region $r \gtrsim 25R_\odot$ by means of internally generated unstable waves has been proposed by several investigators

[Parker, 1958 a, b, 1963; Scarf et al., 1967; Kennel and Scarf, 1968; Hundhausen, 1968; Forslund, 1970]. Since only a small fraction of the total energy is required to raise the proton temperature in this region, solution points in Figures 1 and 2 lying below the empirical results can also be raised approximately vertically by the application of an internally generated heat source; i.e., the corresponding v_E, n_E and T_{pE} will not change appreciably from the case when an equivalent external heat source is applied. It is clear that we can not point to any factor or factors in the present analysis that would rule out the need for heating beyond $25R_\odot$ or, if such heating is necessary, whether or not it is derived from an internally or externally generated source or both. We only argue that it is possible to account for the observed relation between v_E and T_{pE} by application of an external energy source inside the heleocentric radius of about $25R_\odot$ and that the corresponding densities n_E are desirably lower than those resulting from an "extended" or "double-humped" heat source.

In addition to the above internal sources operative over $r \gtrsim 25R_\odot$, Forslund [1970] has shown that an internally generated proton heat source is possible inside $25R_\odot$. He pointed out that the expected skewing of the electron distribution, due to the high rate of thermal conduction, can be responsible for exciting unstable ion-acoustic waves leading to turbulence from which protons can be heated through linear and non-linear Landau damping and collisional damping of the waves on the ions. The inner

boundary for this mechanism occurs where $T_e/T_p \gtrsim 7$, which can take place as close as $r \simeq 10R_\odot$ when the conditions of the HS model prevail. However, when heating occurs, the inner boundary will move outward to satisfy $T_e/T_p \gtrsim 7$. Forslund has also pointed out that such ion-acoustic turbulence should lead to a reduction in the thermal conduction coefficient.

We have argued that energy must be added to the system to account for the observed high speed streams. We do not expect that a reduction in the electron thermal conduction coefficient at $r \gtrsim 10R_\odot$, as suggested by Forslund, can effect an increase in the total energy flux. It seems unlikely that more energy will be drawn out through the base, say, by a possible increase in conduction flux at the base, when the conductive coefficient is reduced at $r \gtrsim 10R_\odot$. However, the relative merits of external and internal energy sources can not be conclusively evaluated until the macroscopic effects of the latter have been quantitatively investigated.

ACKNOWLEDGEMENTS

The authors wish to thank Drs. L. F. Burlaga, P. Cassen, D. W. Forslund, A. J. Hundhausen, and K. W. Ogilvie for useful discussions during the course of this investigation. We also express our thanks to Mr. J. Bredekamp for assistance with the numerical computations.

REFERENCES

Allen, C.W., Astrophysical Quantities, p. 176, Athlone Press, London, 1963.

Axford, W.I., Observations of the interplanetary plasma, Space Sci. Rev., 8, 331, 1968.

Barnes, A., Collisionless damping of hydromagnetic waves, Phys. Fluids, 9, 1483, 1966.

Barnes, A., Collisionless heating of the solar wind plasma, 2, Application of the theory of plasma heating by hydromagnetic waves, Astrophys. J., 155, 311, 1969.

Blackwell, D.E., A study of the outer solar corona from a high altitude aircraft at eclipse of 1954, June 30, Monthly Notices Roy. Astron. Soc., 116, 57, 1956.

Braginskii, S.I., Transport processes in a plasma, in Reviews of Plasma Physics, 1, edited by M.A. Leontovich, pp. 205-311, Consultants Bureau, New York, 1965.

Brandt, J.C., R.W. Michie, and J.P. Cassinelli, Interplanetary gas 10. Coronal temperatures, energy deposition, and solar wind, Icarus, 4, 19, 1965.

Brandt, J.C., C. Wolff and J.P. Cassinelli, Interplanetary gas. 16. A calculation of the angular momeutum of the solar wind, Astrophys. J., 156, 1117, 1969.

Burlaga, L.F., and K.W. Ogilvie, Heating of the solar wind, Astrophys. J., 159, 659, 1970.

Coleman, P.J., Jr., Turbulence, Viscosity, and dissipation in the solar-wind plasma, Astrophys. J., 153, 371, 1968.

Eviatar, A., and M. Schulz, Ion-temperature anisotropies and the structure of the solar wind, to be published, 1970.

Forslund, D.W., Instabilities associated with heat conduction in the solar wind and their consequences, J. Geophys. Res., 75, 17, 1970.

Fredricks, R.W., Electrostatic heating of solar wind ions beyond 0.1 AU, J. Geophys. Res., 74, 2919, 1969.

Gentry, R.A., and A.J. Hundhausen, A solar wind model with magnetically inhibited heat conduction, EOS, Trans. Am. Geophys. Union, 50, 302, 1969.

Gringauz, K.I., V.V. Bezrukikh, and L.S. Musatov, Book of Abstracts, Inter-Union Symp. on Solar Terrestrial Phys., Belgrade.

Hartle, R.E., and P.A. Sturrock, Two-fluid model of the solar wind, Astrophys. J., 151, 1155, 1968.

Hollweg, J.V., Collisionless solar wind. 1. Constant electron temperature, J. Geophys. Res., 75, 1970.

Hundhausen, A.J., Direct observations of solar-wind particles, Space Sci. Rev., 8, 690, 1968.

Hundhausen, A.J., Nonthermal heating in the quiet solar wind, J. Geophys. Res., 74, 5810, 1969.

Jockers, K., Solar wind models based on exopheric theory, Max Planck Institute preprint, MPI-PAE, Astro 28, 1969.

Jokipii, J.R., and L. Davis, Jr., Long-wavelength turbulence and the heating of the solar wind, Astrophys. J., 156, 1101, 1969.

Kennel, C.F., and F.L. Scarf, Thermal anisotropies and electromagnetic instabilities in the solar wind, J. Geophys. Res., 73, 6149, 1968.

Konyukov, M.V., Parker's solar-wind theory, Geomagnetism and Aeronomy, 7, 169, 1967a.

Konyukov, M.V., Parker's solar-wind theory. 2. Flow with a heat source depending on a point, Geomagnetism and Aeronomy, 7, 469, 1967b.

Konyukov, M.V., Plasma emission from the sun with thermal conduction playing a significant role, Geomagnetism and Aeronomy, 8, 489, 1968.

Lazarus, A.J., H.S. Bridge, and J. Davis, Preliminary results from the pioneer 6 M.I.T. plasma experiment, J. Geophys. Res., 71, 3787, 1966.

Michard, R., Densitiés électroniques dans la couronne externe du 25 févier 1952, Ann. Astrophys., 17, 429, 1954.

Montgomery, M.D., S. J. Bame, and A.J. Hundhausen, Solar wind electrons, Vela 4 measurements, J.Geophys. Res., 73, 4999,1968.

Neugebauer, M., and C.W. Snyder, Mariner-2 measurements of the solar wind, in The Solar Wind, edited by R.J. Mackin Jr. and M. Neugebauer, Pergamon, New York, 1966a

Neugebauer, M., and C.W. Snyder, Mariner 2 observations of the solar wind 1. Average properties, J. Geophys. Res., 71, 4469, 1966b.

Newkirk, G., Jr., Structure of the solar corona, in Annual Review of Astronomy and Astrophysics, 5, edited by L. Goldberg, D. Layzer, and J.G. Phillips, pp. 213-266, Annual Reviews, Inc., Palo Alto, 1967.

Noble, L.M. and F.L. Scarf, Conductive Heating of the solar wind. I, Astrophys. J., 138, 1169, 1963.

Parker, E.N., Dynamics of the interplanetary gas and magnetic fields, Astrophys. J., 128, 664, 1958a.

Parker, E.N., Dynamical instability in an anisotropic ionized gas of low density, Phys. Rev., 109, 1844, 1958b.

Parker, E.N., Interplanetary dynamical processes, Interscience, New York, 1963.

Parker, E.N., Dynamical theory of the solar wind, Space Sci. Rev., 4, 666, 1965a.

Parker, E.N., Dynamical properties of stellar coronas and stellar wind. II. The separate existence of subsonic and supersonic solutions, Astrophys. J., 141, 1463, 1965b.

Parker, E.N., Theoretical studies of the solar wind phenomenon, Space Sci. Rev., 9, 325, 1969.

Robbins, D.E., A.J. Hundhausen, and S.J. Bame, Helium in the Solar Wind, J. Geophys. Res., 75, 1178, 1970.

Rogister, A., and C. Oberman, On the kinetic theory of stable and weakly unstable plasma, 1, J. Plasma Phys., 2, 33, 1968.

Scarf, F.L., J.H. Wolfe, and R.W. Silva, A plasma instability associated with thermal anisotropies in the solar wind, J. Geophys. Res., 72, 993, 1967.

Shapiro, A.H., The dynamics and thermodynamics of compressible fluid flow, 1, Ronald, New York, 1953.

Sturrock, P.A., and R.E. Hartle, Two-fluid model of the solar wind, Phys. Rev. Letters, 16, 628, 1966.

Urch, I.H., A model of the magnetized solar wind, Solar Phys., 10, 219, 1969.

Whang, Y.C., and C.C. Chang, An inviscid model of the solar wind, J. Geophys. Res., 70, 4175, 1965.

Wolfe, J.H., R.W. Silva, and M.A. Myers, Observations of the solar wind during the flight of IMP 1, J. Geophys. Res., 71, 1319, 1966.

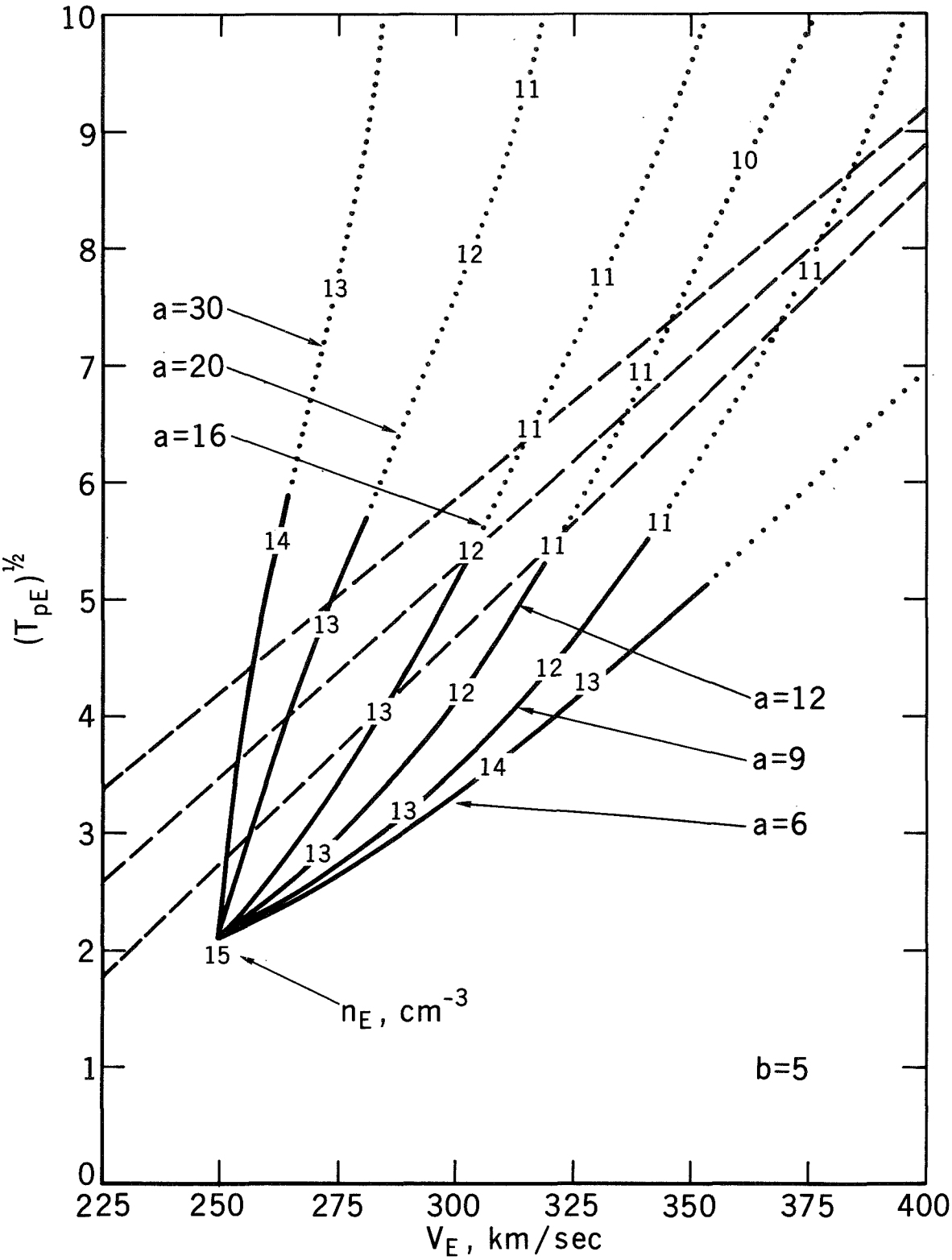

Fig. 1 - The square root of proton temperature T_{pE} at 1AU in kilo-degrees Kelvin versus wind speed v_E in km/sec. Analytical results are given by solid lines (and corresponding dotted lines) with corresponding values of density n_E in cm^{-3} indicated at selected points. For comparison, the empirical results of Burlaga and Ogilvie are shown by dashed lines.

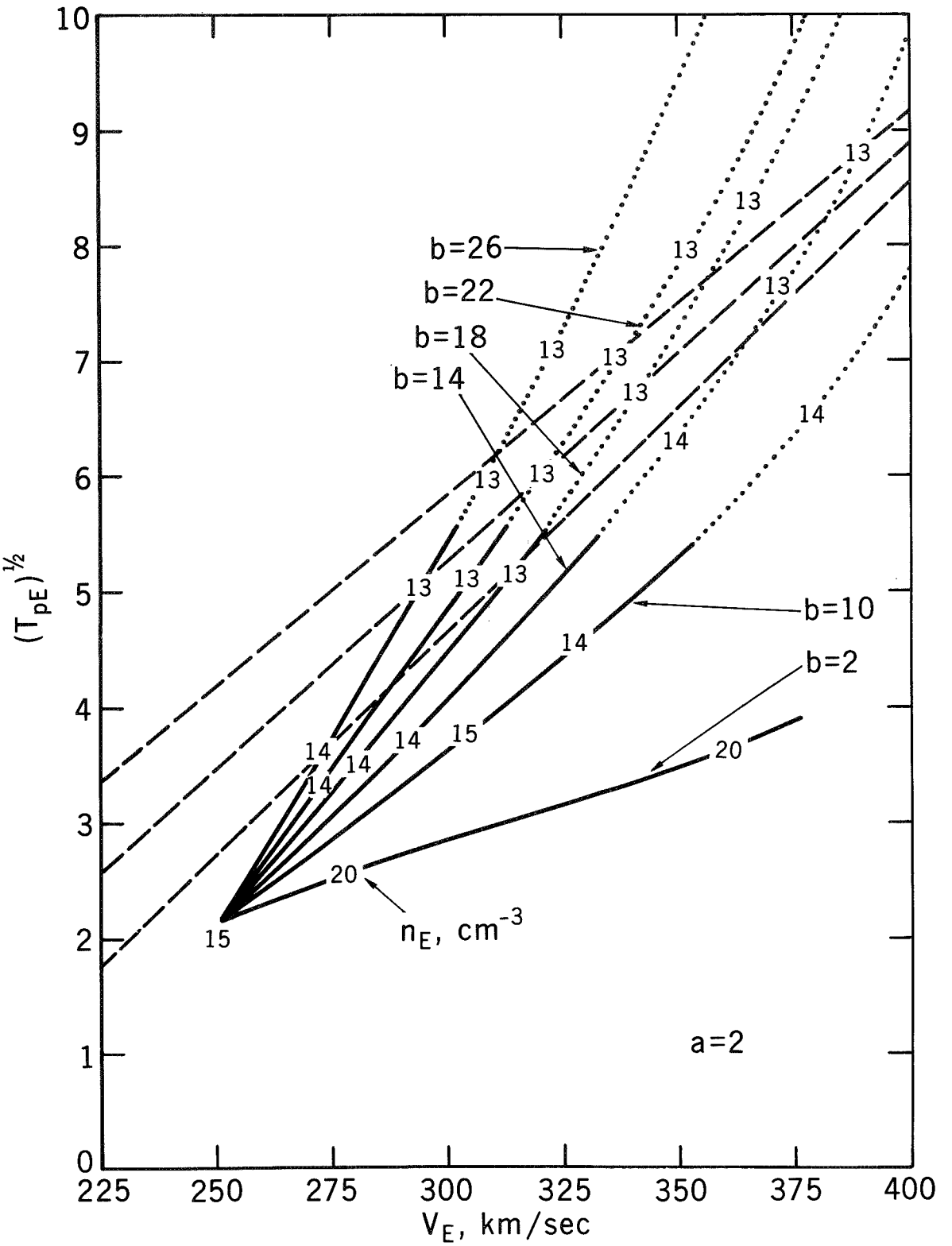

Fig. 2 - The square root of proton temperature T_{pE} at 1AU in kilo-degrees Kelvin versus wind speed v_E in km/sec. Analytical results are given by solid lines (and corresponding dotted lines) with corresponding values of density n_E in cm^{-3} indicated at selected points. For comparison, the empirical results of Burlaga and Ogilvie are shown by dashed lines.

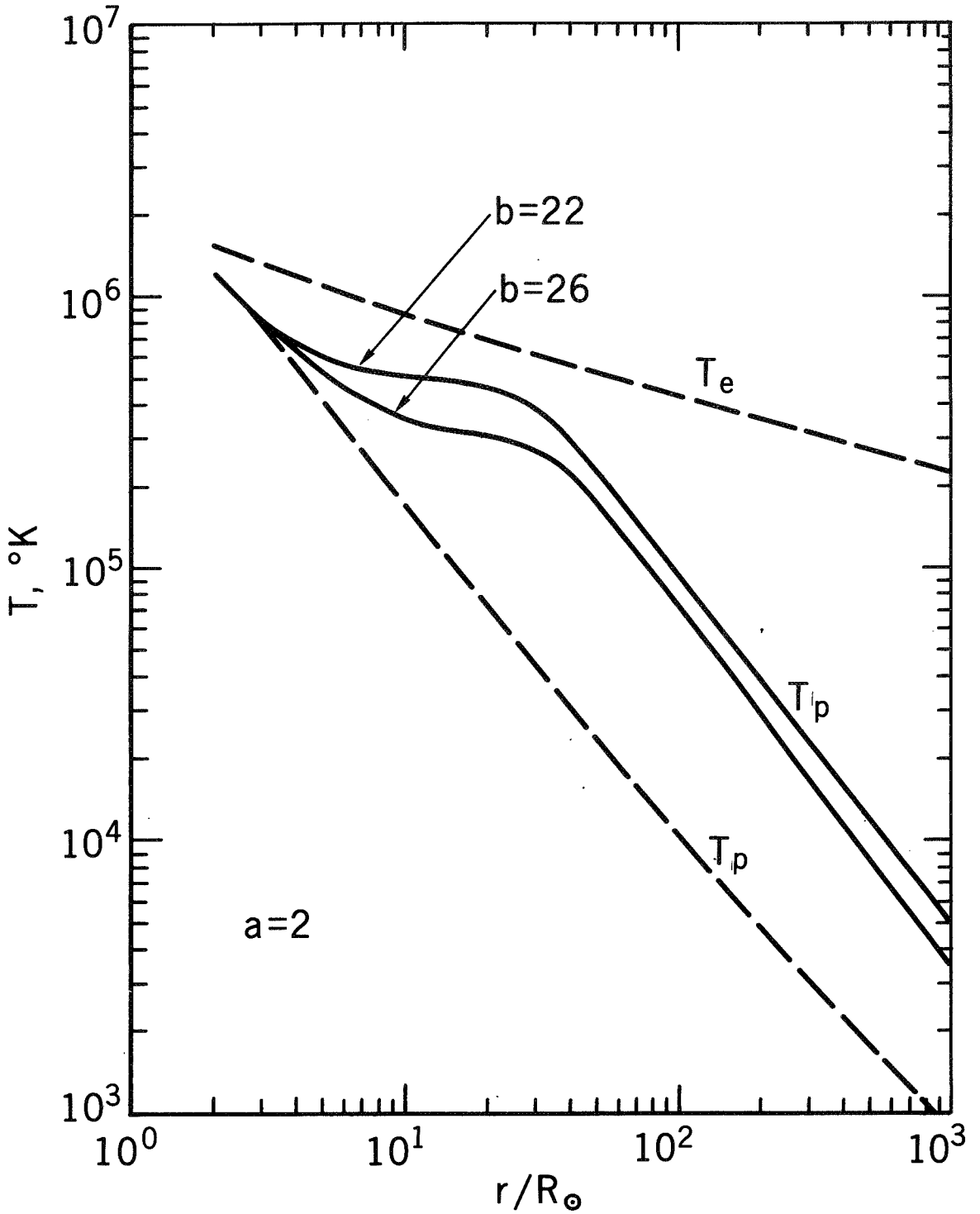

Fig. 3 - Proton temperature T_p and electron temperature T_e versus radius r. Temperature profiles resulting from heat sources characterized by a=2, b=22, $D_o=6 \times 10^{-9}$, and a=2, b=26, $D_o=3 \times 10^{-9}$ are given by solid lines. For comparison, corresponding results of HS model are shown by dashed lines.

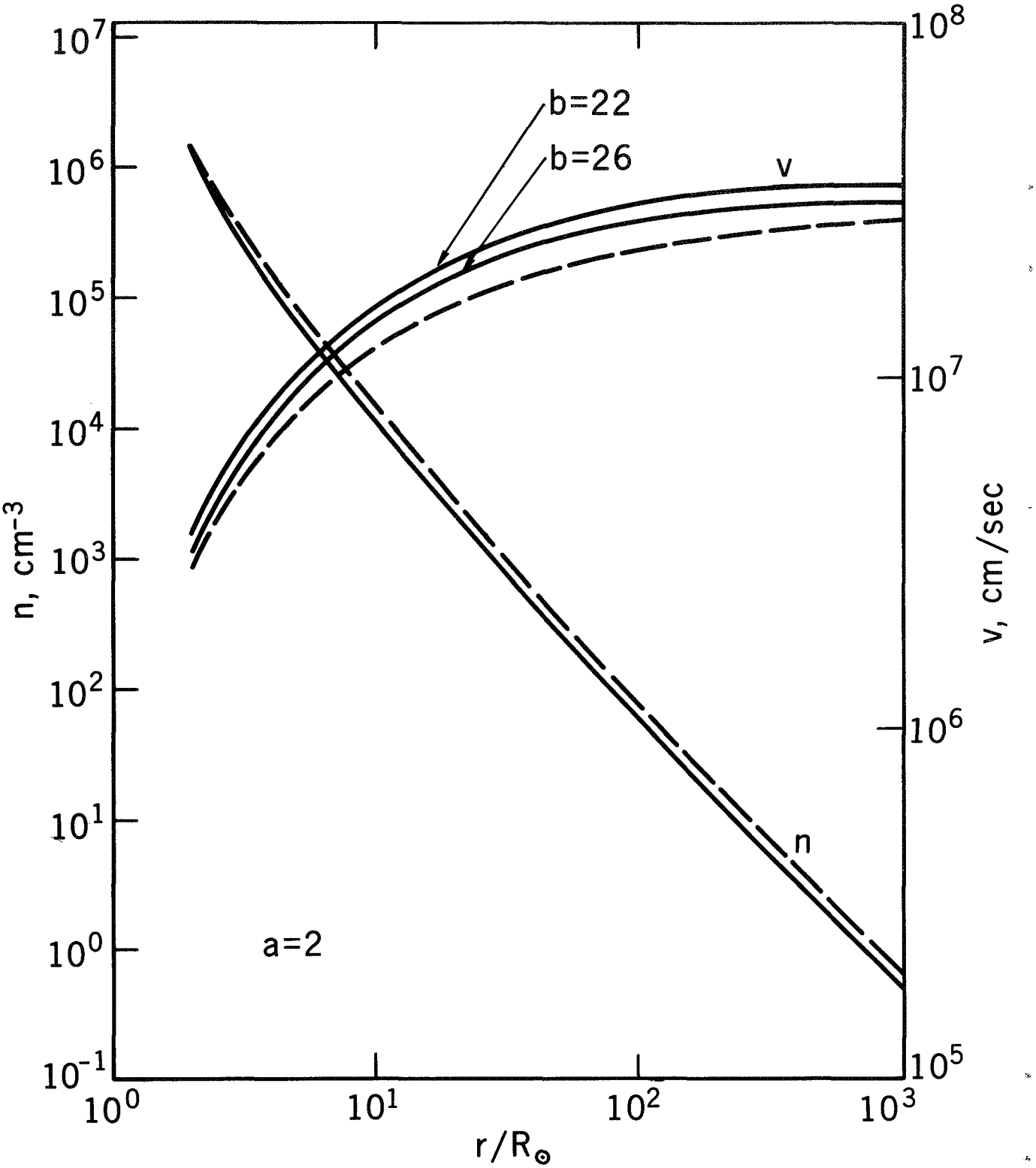

Fig. 4 - Wind speed v and density n versus radius r. Density and wind speed profiles resulting from heat sources characterized by a=2, b=22, D_o=6 x 10^{-9}, and a=2, b=26, D_o=3 x 10^{-9} are given by solid lines. For comparison, corresponding results of HS model are shown by dashed lines.

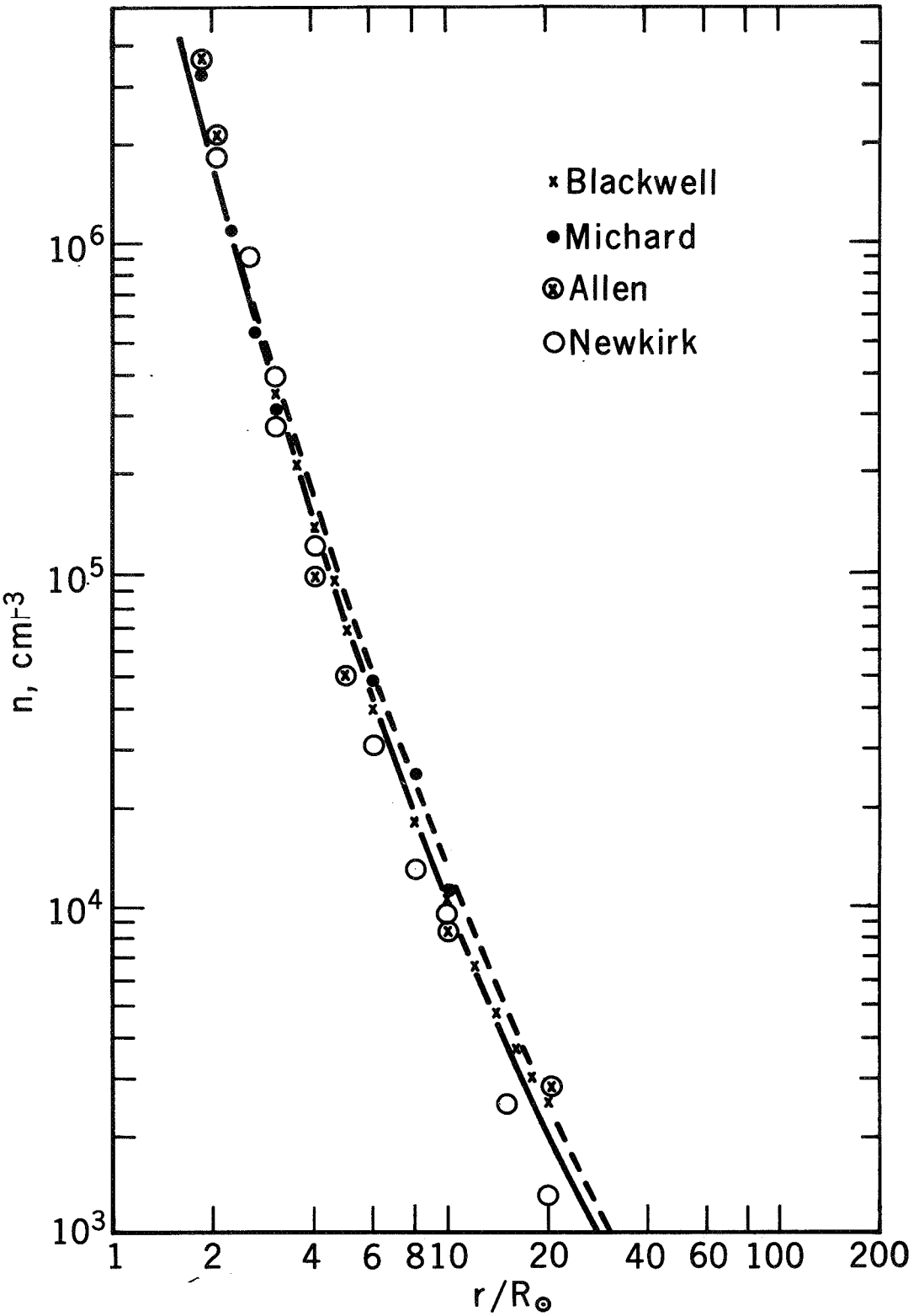

Fig. 5 - Density n versus radius r. The solid line corresponds to the density profile of Fig. 3, given by a solid line. The observational results of Blackwell, Michard, Allen and Newkirk are indicated. For comparison, the density profiles of HS model are shown by dashed lines.

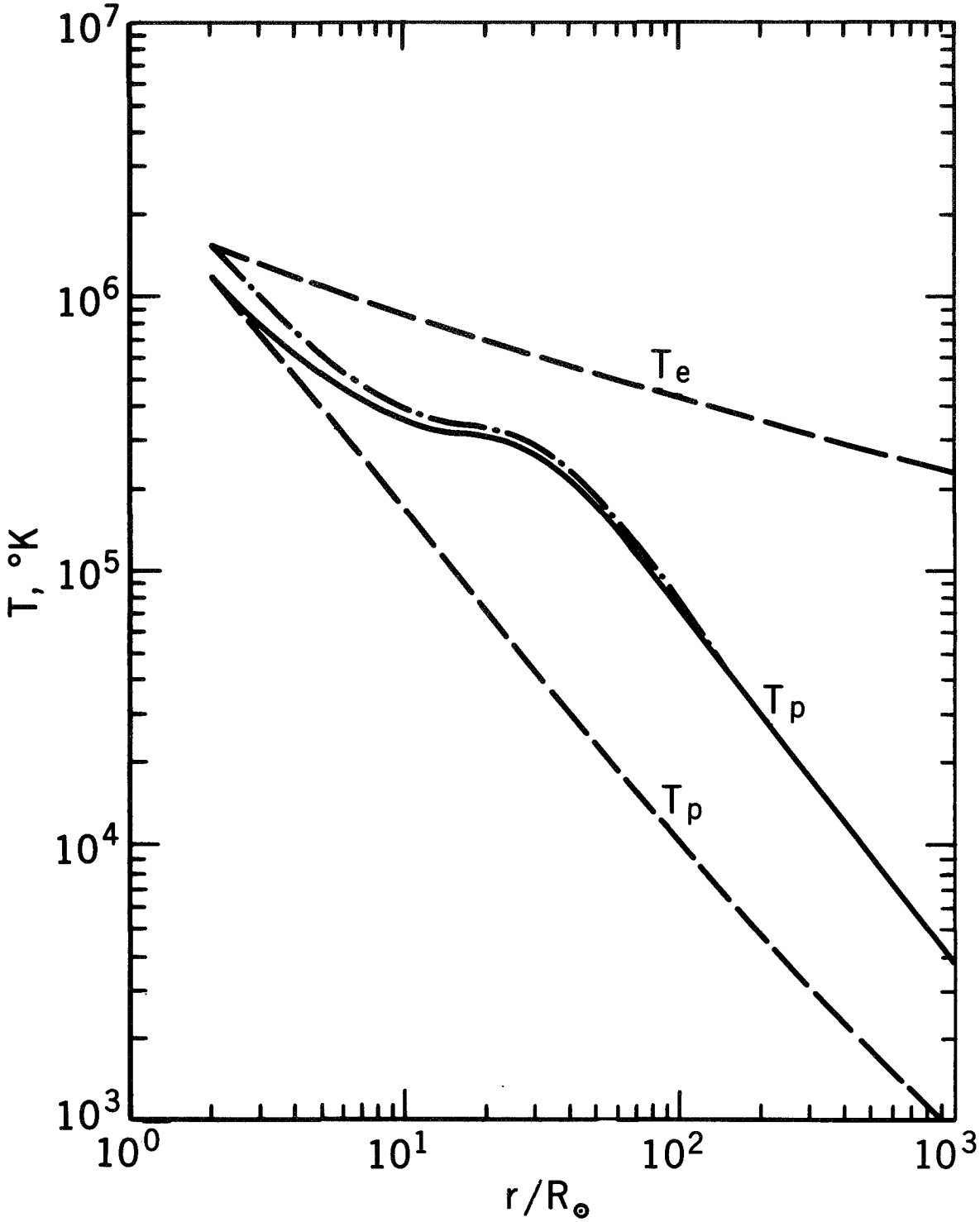

Fig. 6 - Proton temperature T_p and electron temperature T_e versus radius r. Solid and dot-dashed lines correspond to a heat source characterized by a=2, b=26, and $D_o=3 \times 10^{-9}$. Solid line corresponds to $T_{po}=1.2 \times 10^6$ °K and dot-dashed line to $T_{po}=1.5 \times 10^6$ °K. For comparison, corresponding results of HS model are shown by dashed lines.

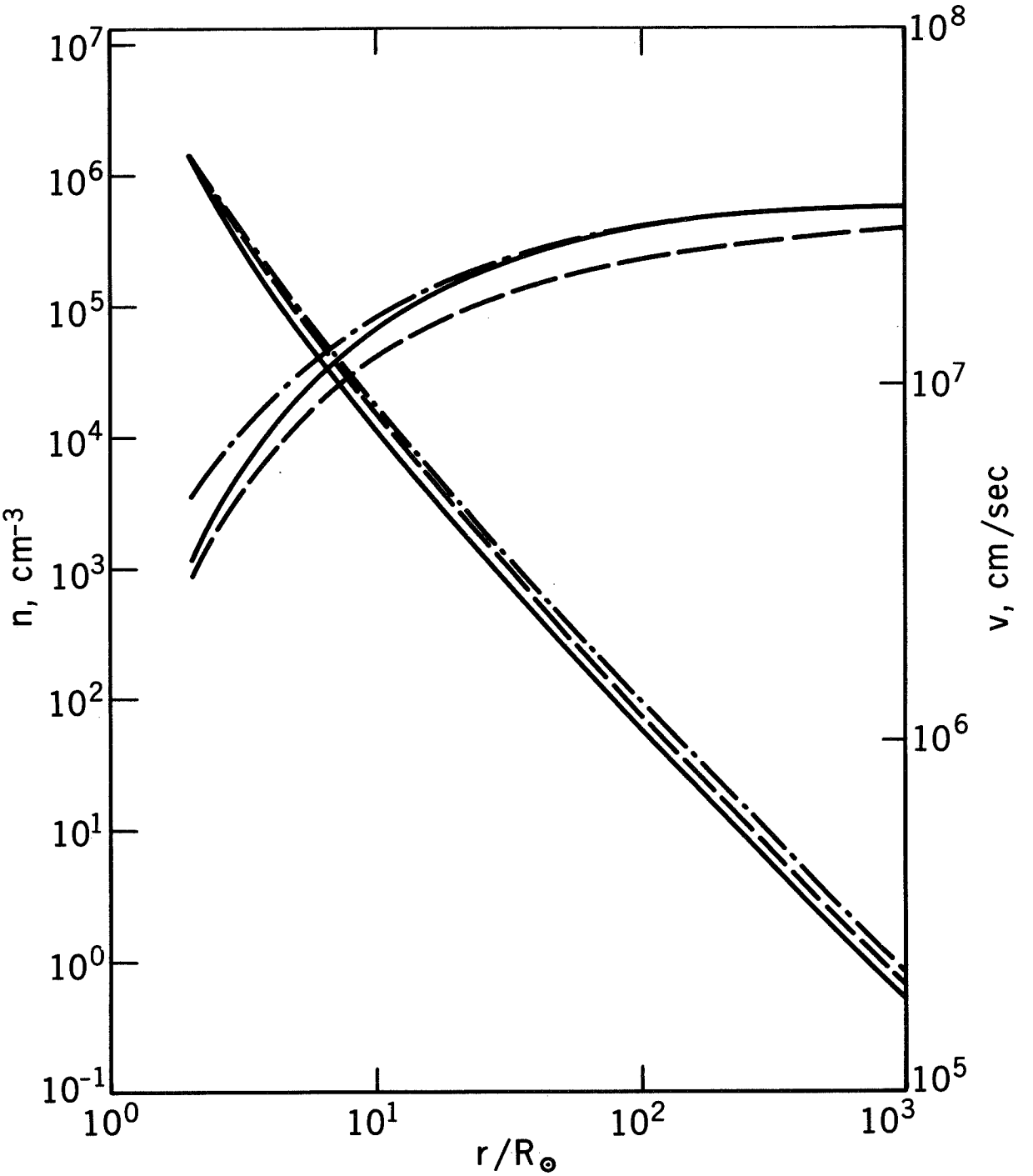

Fig. 7 - Wind speed v and density n versus radius r. Solid and dot-dashed lines correspond to a heat source characterized by a=2, b=26, and $D_o = 3 \times 10^{-9}$. Solid lines correspond to $T_{po} = 1.2 \times 10^6$ °K and dot-dashed lines to $T_{po} = 1.5 \times 10^6$ °K. For comparison, corresponding results of HS model are shown by dashed lines.